Electronic Supplementary Material (ESI) for Polymer Chemistry.

Supporting Information

to

Polymer brush guided templating on well-defined rod-like cellulose nanocrystals

Maria Morits,[a,d] Ville Hynninen,[a] Nonappa,[a,b] Antoine Niederberger,[d] Olli Ikkala,[a,b] André H. Gröschel,[c] Markus Müllner[d,e,*]

[a] Department of Applied Physics, Aalto University, FI-02150 Espoo, Finland.

[b] Department of Bioproducts and Biosystems, Aalto University, FI-02150, Espoo, Finland.

[c] Physical Chemistry and Centre for Nanointegration Duisburg-Essen (CENIDE), University of Duisburg-Essen, D-45127 Essen, Germany.

[d] Key Centre for Polymers and Colloids, School of Chemistry, The University of Sydney, Sydney, New South Wales 2006, Australia.

[e] Australian Institute for Nanoscale Science and Technology, The University of Sydney, Sydney, New South Wales 2006, Australia.

E-mail: markus.muellner@sydney.edu.au

S1 CNC ξ-potential

The ξ-potential of unmodified CNC was < -50 mV.

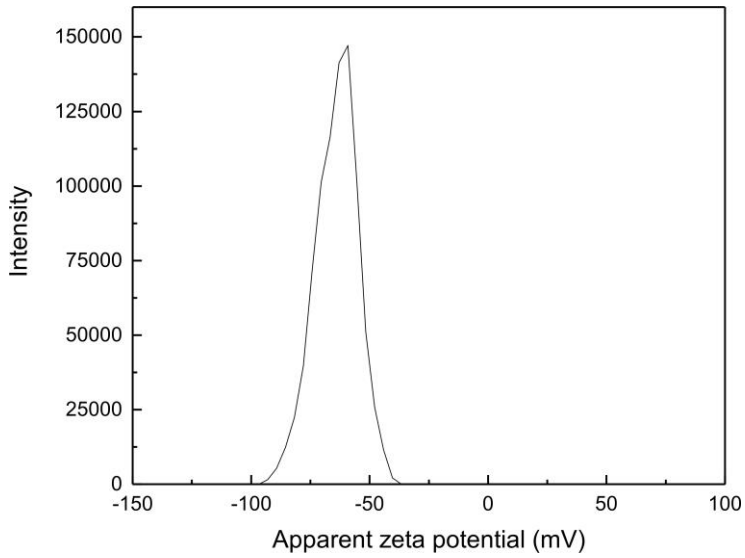

Fig. S1 ξ-potential of CNCs prior to modification.

S2 CNC length distribution

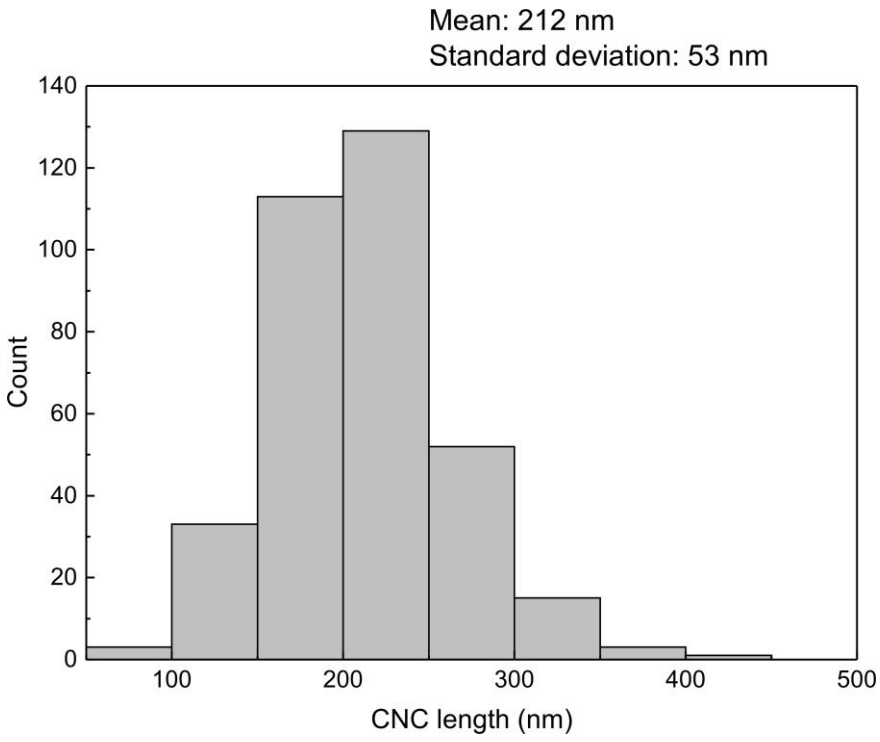

Fig. S2 CNC length distribution as derived from TEM images.

S3 GPC of sacrificial PDMAEMA

PDMAEMA was polymerized from CNC-Br in presence of sacrificial initiator ethyl bromoisobutyrate.

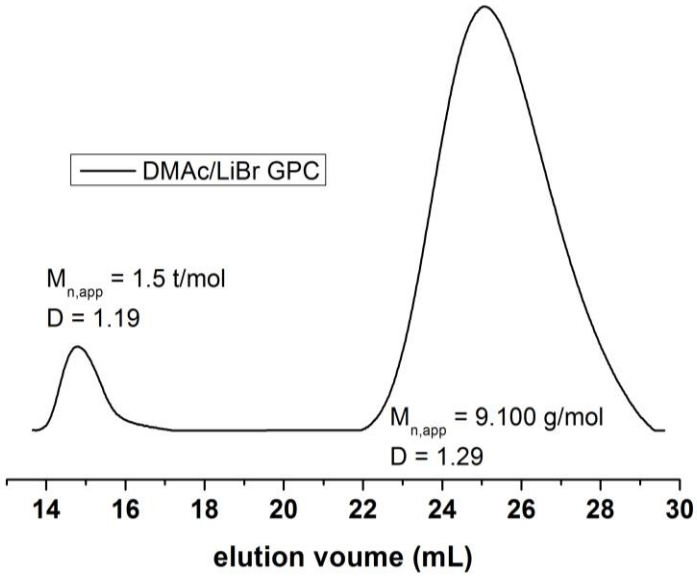

Fig. S3 GPC elution trace of free PDMAEMA in DMAc. The right peak corresponds to linear PDMAEMA ($M_{n,app}$ = 9,100 g/mol) whereas the left peak is CNC-*g*-PDMAEMA ($M_{n,app}$ = 1,500,000 g/mol) which also passed through the filter during sample preparation.

S4 FT-IR analysis

Fig. S4A shows a magnified version of the FT-IR analysis of the CNC modification and polymer grafting from the manuscript (see discussion and Fig. 2B). Fig. S4B shows FT-IR comparison of as-synthesised and calcined hybrids. The nanomaterials have pronounced peaks corresponding to silica. The spectrum of the as-synthesized hybrid indicated the presence of the carbonyl groups of PDMAEMA (top, black spectrum). After calcination of the hybrids all organic matter was removed, resulting in the disappearance of the carbonyl group (bottom, blue spectrum).

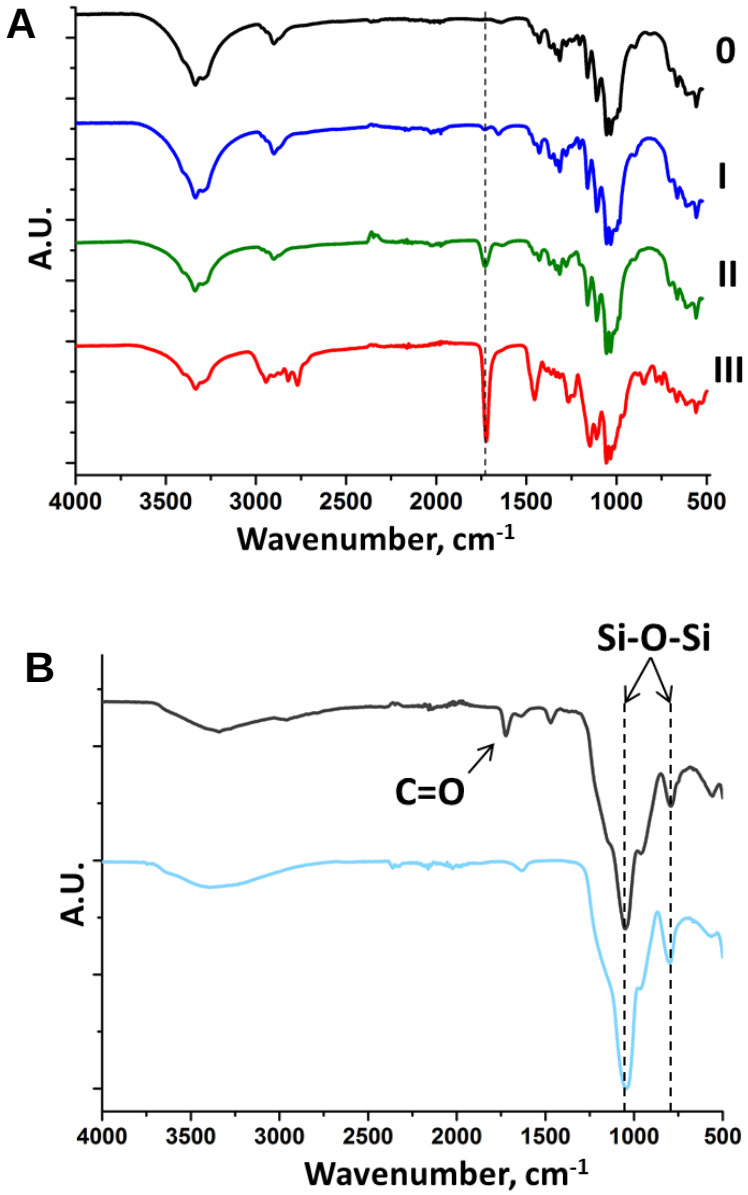

Fig. S4 FT-IR analyses of A) CNC modifications resulting in an increase of the carbonyl peak and a small shift relative to the carbonyl signal of CNC-Br and B) as-synthesised hybrid (top, black line) and calcined (bottom, blue line) nanomaterials.

S5 AFM cross-section analysis of CNC-Br

Fig. S5 shows the cross-sections of the marked CNC-Br in Fig. 4A of the manuscript. The y-axis is adjusted to 40 nm to warrant direct comparison to the cross-sections of the polymer grafted CNCs in Fig. S6.

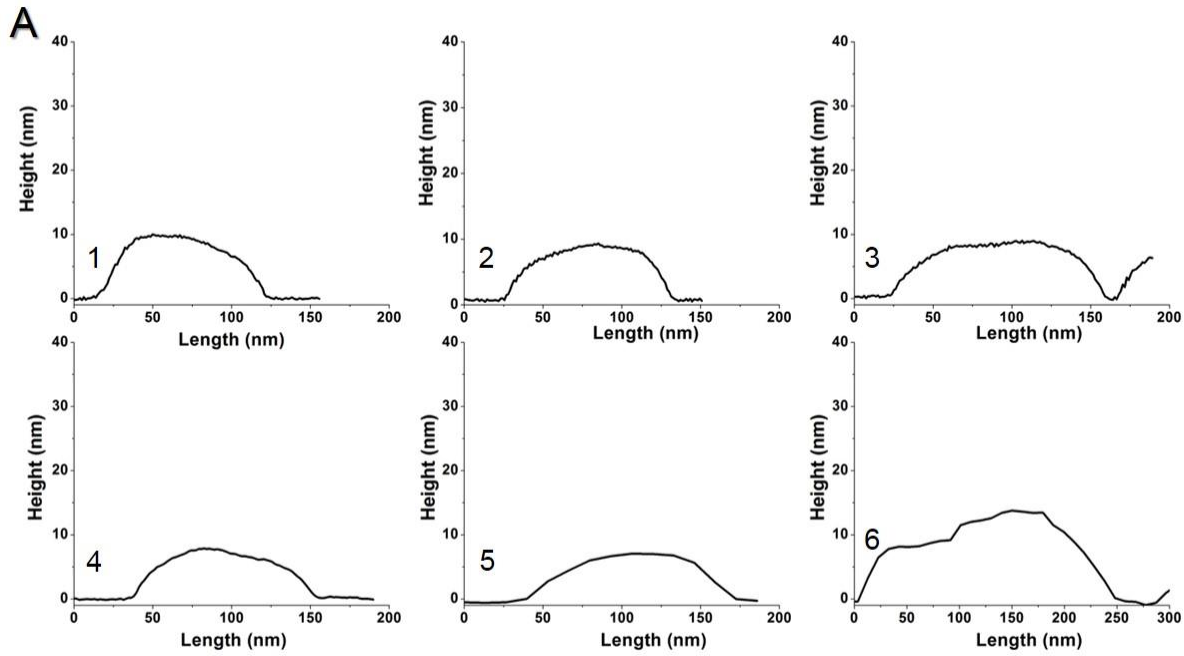

Fig. S5 AFM height cross-sections of CNC-Br on mica. The area of the cross-section is numbered an indicated in Fig. 4A in the manuscript.

S6 AFM images of CNC-*g*-PDMAEMA

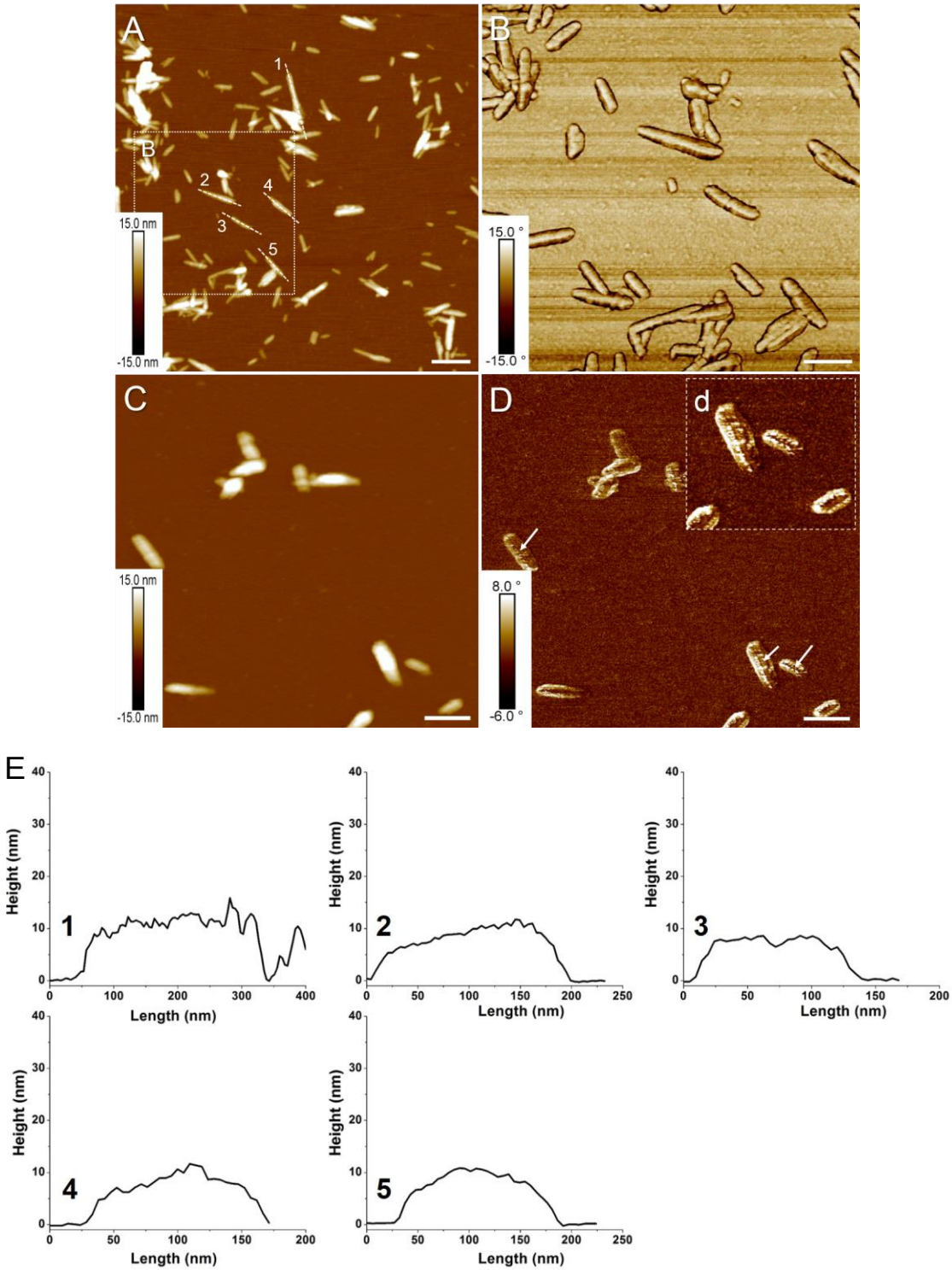

Fig. S6 AFM height (A/C) and phase images (B/D) of CNC-*g*-PDMAEMA$_{25}$ and CNC-*g*-PDMAEMA$_{50}$, respectively. Samples were deposited from methanol onto freshly cleaved mica. Scale bars are 200 nm (A/C/D) and 100 nm (B). Dashed lines 1-5 in A) correspond to the AFM height profiles in E). Arrows in D) indicate the CNC core.

S7 AFM cross-section analyses

Fig. S7 shows the same cross-sectional analysis that is shown in Fig.S5. However, the y-axis is adjusted to 80 nm to allow a direct comparison across all cross-sections derived from Fig. 4A-D of the manuscript.

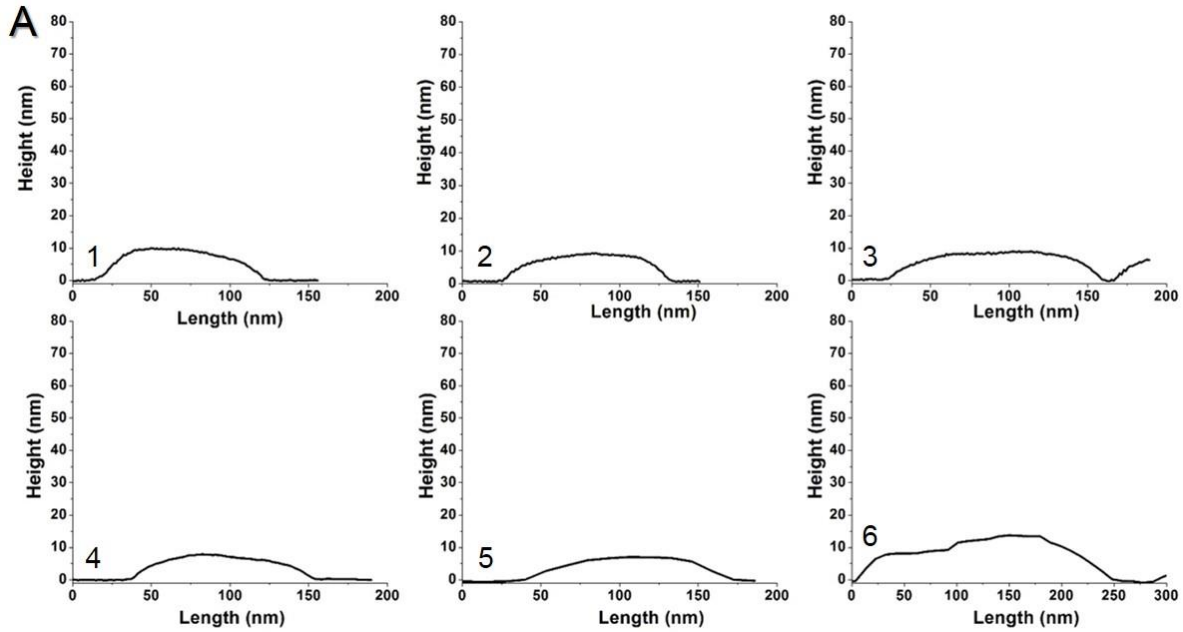

Fig. S7-A AFM height cross-sections of CNC-Br on mica. The area of the cross-section is numbered an indicated in Fig. 4A in the manuscript.

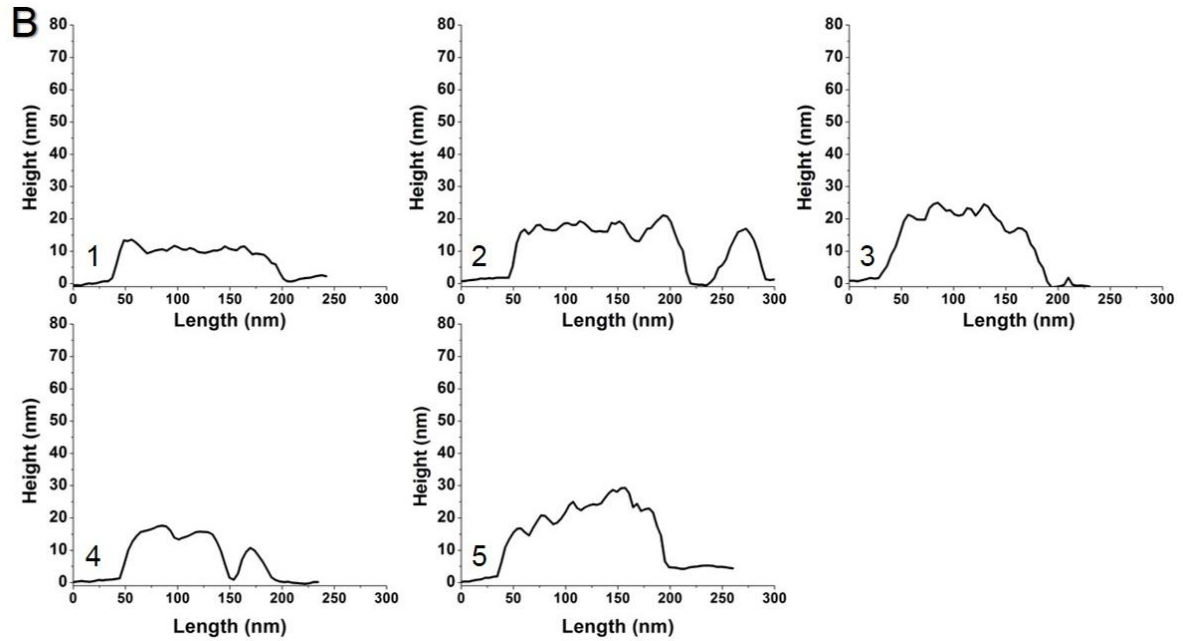

Fig. S7-B AFM height cross-sections of SiO_2@CNC-*g*-$PDMAEMA_{10}$ on mica. The area of the cross-section is numbered an indicated in Fig. 4B in the manuscript.

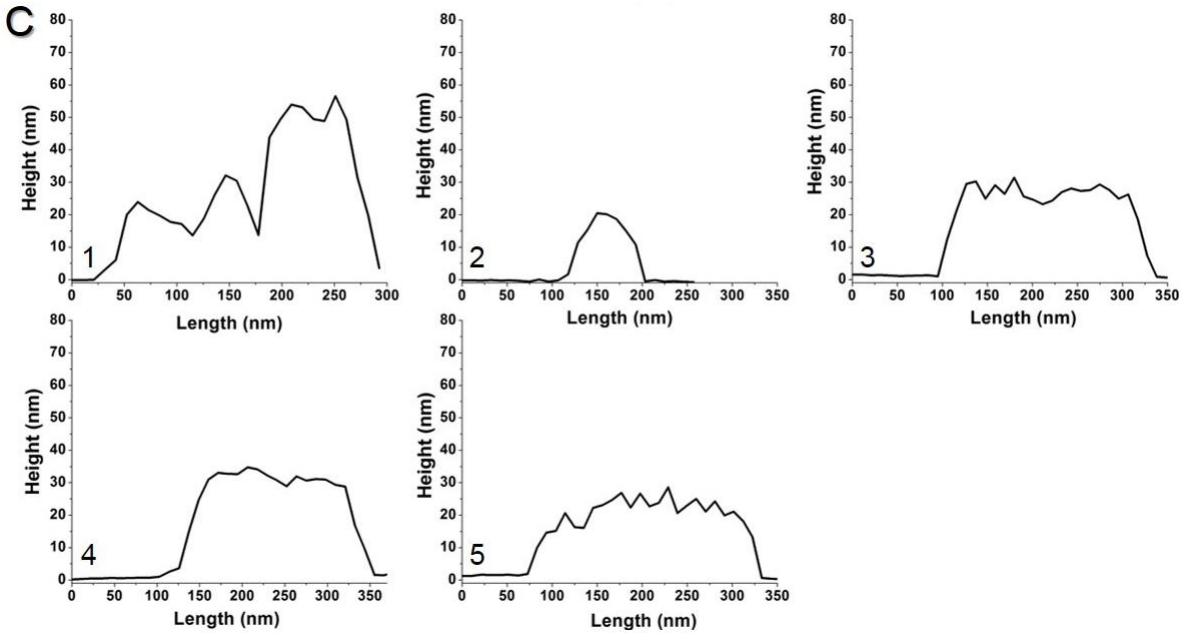

Fig. S7-C AFM height cross-sections of SiO_2@CNC-*g*-$PDMAEMA_{25}$ on mica. The area of the cross-section is numbered an indicated in Fig. 4C in the manuscript.

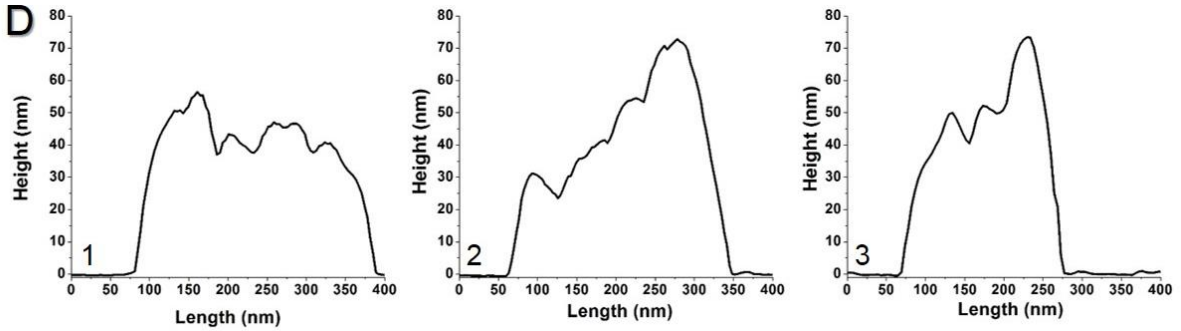

Fig. S7-D AFM height cross-sections of SiO_2@CNC-*g*-$PDMAEMA_{50}$ on mica. The area of the cross-section is numbered an indicated in Fig. 4D in the manuscript.

S8 TEM analyses of SiO_2@CNC-*g*-PDMAEMA

The diameter of both the entire hybrid as well as the core can be visualised and measured using grey-scale analyses.

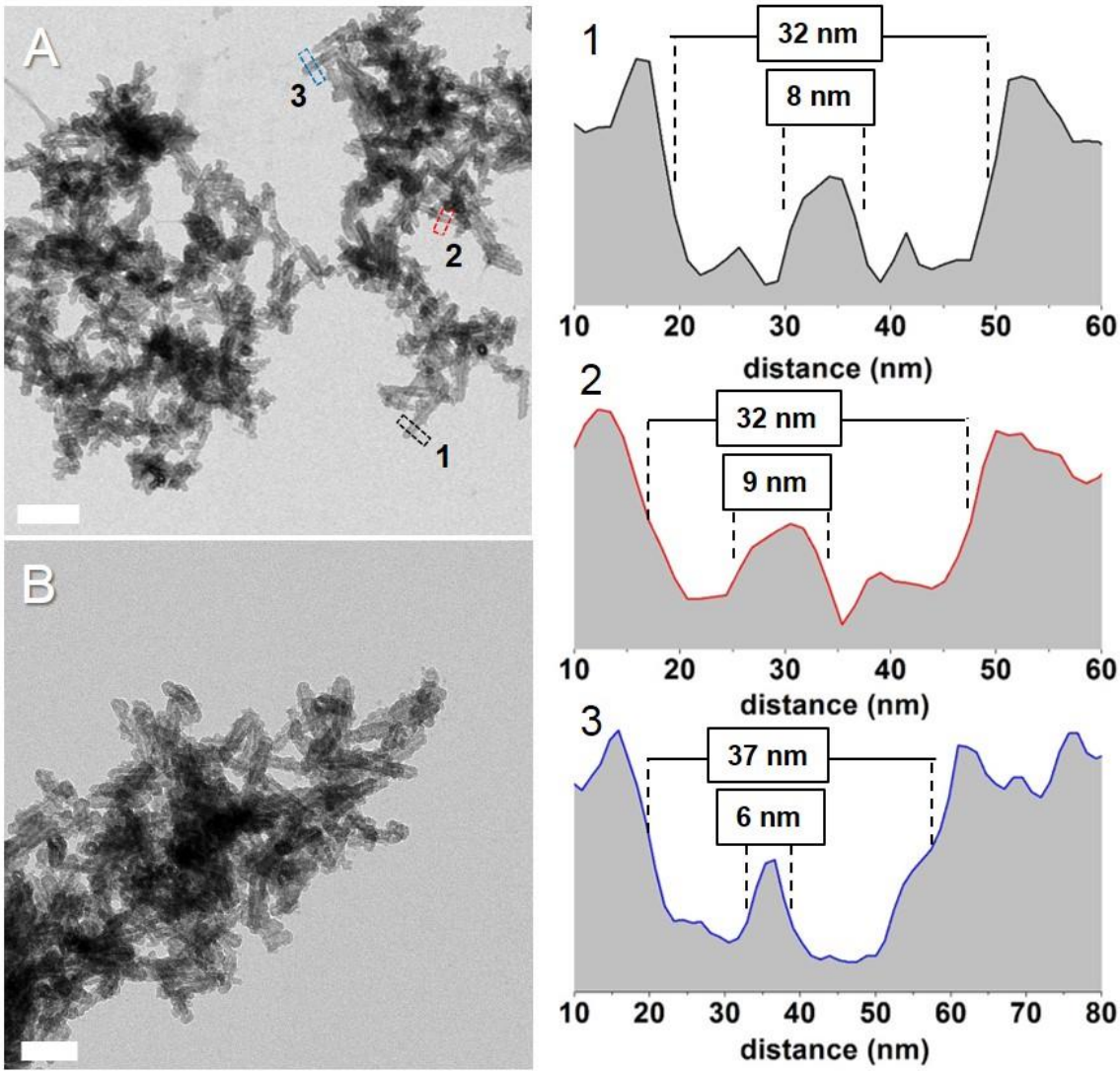

Fig. S8 TEM images of SiO_2@CNC-*g*-PDMAEMA$_{15}$. Scale bars are 100 nm (A) and 200 nm (B). The right panel presents the cross-sectional profile of the indicated areas in (A) and highlight the nanotubular morphology.

S9 Meso-pore distribution

Pore distribution derived from N_2-physisoprtion experiments reveal the average pore width/diameter of the calcined hollow nanorods (which matched the measured diameters of the pristine CNCs).

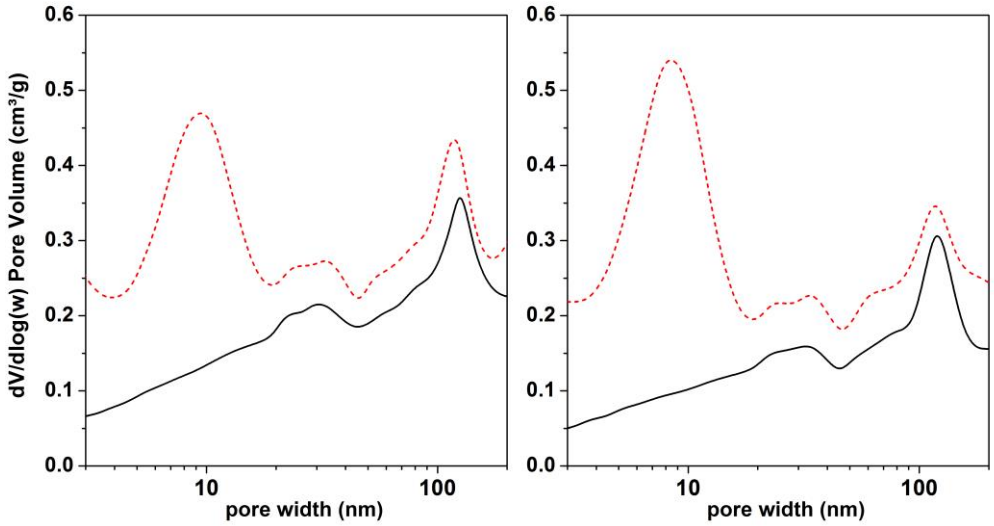

Fig. S9 Width distribution of meso-pores of SiO_2@CNC-*g*-$PDMAEMA_{25}$ (left) and SiO_2@CNC-*g*-$PDMAEMA_{15}$ (right) before (black solid line) and after (red dashed line) calcination.